

ARTICLE



Detection ability of corneal biomechanical parameters for early diagnosis of ectasia

Mohammad-Reza Sedaghat¹, Hamed Momeni-Moghaddam²✉, Javad Heravian³, Atiyeh Ansari³, Helia Shayanfar¹ and Majid Moshirfar^{4,5,6}

© The Author(s), under exclusive licence to The Royal College of Ophthalmologists 2022

PURPOSE: To assess the detection ability of corneal biomechanical parameters for early diagnosis of ectasia.

METHODS: This retrospective descriptive-analytical study included 134 normal eyes (control group) from 134 healthy subjects and 128 eyes with asymmetric contralateral corneal ectasia with normal topography (ACE-NT, study group) from 128 subjects with definite keratoconus in the opposite eye. Placido-disk-based corneal topography with TMS-4, Scheimpflug corneal tomography with Pentacam HR, and corneal biomechanical assessment with Corvis ST and ocular response analyzer (ORA) were performed. A general linear model was used to compare Corvis ST and ORA biomechanical parameters between groups, while central corneal thickness (CCT) and biomechanically corrected intraocular pressure (bIOP) were considered covariates. Receiving operator sensitivity curve (ROC) analysis was used to determine the cut-off point with the highest sensitivity and specificity along with the area under the curve (AUC) for each parameter.

RESULT: All parameters of Corvis ST and ORA showed a statistically significant difference between the two groups except for the first ($P = 0.865$) and second ($P = 0.226$) applanation lengths, and deformation amplitude ($P = 0.936$). The discriminative analysis of corneal biomechanical showed that the highest accuracy for the classic, new, and combined parameters of Corvis ST was related to HCR (AUC: 0.766), IR & DAR (0.846), and TBI (0.966), respectively. Using ORA, the corneal resistance factor (0.866) had a higher detection ability than corneal hysteresis (0.826).

CONCLUSIONS: TBI has the best accuracy and the highest effect size for differential diagnosis of normal from ACE-NT eyes with a cut-off point of 0.24.

Eye (2023) 37:1665–1672; <https://doi.org/10.1038/s41433-022-02218-9>

INTRODUCTION

Keratoconus (KCN) is a bilateral, typically asymmetric, and non-inflammatory corneal degeneration associated with a corneal protrusion, progressive thinning of the corneal stroma, myopia, irregular corneal astigmatism, increase of higher-order aberrations, reduced and fluctuated visual function [1–3]. The term subclinical keratoconus describes the very early preclinical stage of this disease that can only be detected with aid of corneal imaging corneal topo/tomography techniques. Other interchangeable terms used in the literature include forme fruste keratoconus, very asymmetric corneal ectasia with normal topography (VAE-NT), subclinical keratoconus, and keratoconus suspect that describe the early stages of keratoconus [3, 4]. It may be argued that a better phrase than VAE-NT is needed because these eyes have normal topo/tomography, and the only distinctive parameter for them is the abnormal ectatic contralateral eye. Therefore, asymmetrical contralateral cornea ectasia with normal topography (ACE-NT) seems a better alternative to VAE-NT.

Studies investigating keratoconus in terms of refractive, aberrometric, topo/tomographic, and biomechanical characteristics have

reported that changes in the biomechanical behavior of the cornea can reveal signs of ectasia even before they appear on topo/tomographic maps [5–7].

Corneal biomechanical failure is considered a contributing factor in the development of this disease following changes in the corneal geometrical properties and reduced visual quality [8, 9]. With the development of corneal refractive surgery methods, the evaluation of corneal biomechanical properties to reduce the risk of iatrogenic ectasia in the long term has attracted much attention. The unrecognized very early stage of keratoconus is a leading cause of iatrogenic ectasia after laser in situ keratomileusis (LASIK) [10]. Assessing the corneal biomechanical properties appear as one of the main approaches in the early detection of keratoconus. A better understanding of these properties of the cornea might help the detection of eyes at risk for developing ectasia after refractive surgery [11–13].

Two devices currently available for in vivo clinical assessment of corneal biomechanical parameters in the clinic are the ocular response analyzer (ORA, Reichert Ophthalmic Instruments, Buffalo, NY, USA) and Corvis ST (Oculus Optikgerate GmbH, Wetzlar,

¹Eye Research Center, Mashhad University of Medical Sciences, Mashhad, Iran. ²Health Promotion Research Center, Zahedan University of Medical Sciences, Zahedan, Iran.

³Department of Optometry, School of Paramedical Sciences, Mashhad University of Medical Sciences, Mashhad, Iran. ⁴Hoopes Vision Research Center, Hoopes Vision, 11820S. State St. #200, Draper, UT 84020, USA. ⁵John A. Moran Eye Center, University of Utah School of Medicine, Salt Lake City, UT, USA. ⁶Utah Lions Eye Bank, Murray, UT, USA.

✉email: hmomeni_opt@yahoo.com

Received: 23 May 2022 Revised: 12 July 2022 Accepted: 12 August 2022

Published online: 29 August 2022

Germany) [14]. Although some corneal biomechanical parameters in normal eyes and eyes with very asymmetric corneal ectasia with normal or relatively normal corneal topography have been investigated; however, there is a need for further studies to demonstrate the diagnostic ability of the parameters provided by these two available devices for in vivo evaluations. Therefore, the present study was designed to assess the diagnostic ability of corneal biomechanical parameters using both currently available devices for in vivo clinical evaluation of corneal biomechanical parameters (ORA & Corvis ST) to distinguish normal eyes from asymmetric contralateral corneal ectasia with normal topography (ACE-NT) in a larger sample in to provide more evidence for the role of these parameters as well as the cut-off points of each of them.

PATIENTS AND METHODS

Subjects

This retrospective descriptive-analytical study included 262 eyes (134 eyes in the control/normal group and 128 eyes in the study group). The control group was 134 normal eyes from 134 healthy subjects. There were 128 cases with definite keratoconus in one eye and no signs of ectasia on the topographic map (indices or pattern) in the opposite eye, these eyes were labeled as asymmetric contralateral corneal ectasia with normal topography (ACE-NT) eye and were selected as the study group. A pilot study was conducted to calculate the sample size based on the mean and standard deviation of corneal biomechanical parameters obtained in 20 eyes examined in each group, considering the 95% confidence interval and 80% statistical power.

Definite or clinical ectasia keratoconus was diagnosed and confirmed by an experienced fellowship of the cornea (MRS) based on slit-lamp findings (e.g. Fleischer ring, Vogt striae), scissoring retinoscopic reflex, and abnormal sagittal (axial) corneal curvature map (e.g. asymmetric bow-tie with inferior steepening, skewing of the steepest radial axis (SRAX) with asymmetric bow-tie), abnormal elevation values on anterior (>15 microns) and posterior (>20 microns) elevation maps with an 8.0 mm floating best fit sphere (BFS) reference surface, a corneal thinnest point less than 470 microns along with the abnormal patterns on the thickness map, and abnormal thickness progression indices in one eye, while the opposite eyes were considered ACE-NT if they had normal pattern and index (e.g. steep keratometry less than 47.2 diopters, I-S (inferior-superior asymmetry) value less than 1.4, SRAX less than 20 degrees) on the front sagittal curvature map with a normal level on the topographic keratoconus classification (TKC) provided by Pentacam HR [15]. The corneal topography of a patient with normal topography in the right eye, which was considered ACE-NT, and an abnormal topography showing definite keratoconus in the left eye is illustrated in Supplemental Fig. S1.

The aims and objectives of the study were explained to all participants and informed written consent was signed by all subjects. In addition, the study protocol followed the principles of the Declaration of Helsinki at all stages and was approved by the local ethics committee. (Code: IR.MUMS.REC.1399.418)

The control (normal) group was selected from the candidates for refractive surgery referred to Didar Eye Clinic (Mashhad, Iran). Multimodal corneal imaging is performed in addition to the standard ophthalmic examinations to reduce the likelihood of misdiagnosis.

The exclusion criteria in both groups (study/subclinical KCN & control/normal) were central cornea scar, a history of corneal/ocular surgery, ocular diseases, and eye trauma (except keratoconus in the study group on the opposite eye), contact lens wear in the last month, systemic disorders (allergy/atopy, diabetic mellitus, autoimmune, and herpetic diseases), and pregnancy or breastfeeding at the time of assessment.

Assessments

Along with standard ophthalmic examinations, Placido-disk-based corneal topography using the TMS-4 (Tomey Corp, Nagoya, Japan), Scheimpflug corneal tomography using Pentacam HR (Oculus; Wetzlar, Germany), and corneal biomechanical assessments using Corvis ST (Oculus; Wetzlar, Germany) and ocular response analyzer (ORA, Reichert Ophthalmic Instruments, Buffalo, NY, USA) were performed for all participants.

Included variables

Pentacam-derived variables were mean keratometry on both corneal surfaces, maximum keratometry and central corneal thickness (CCT).

Corneal biomechanical parameters obtained from Corvis ST were dynamic corneal response (DCR) parameters provided in the standard and ARV (Ambrosio, Roberts, Vinciguerra) printouts associated with intraocular pressure (IOP) Corvis ST parameters were those related to the first applanation phase (applanation length (AL1) and applanation velocity (AV1)), related to the second applanation phase (AL2, AV2), related to the highest concavity phase (peak distance (PD) or the distance between the two peaks), deformation amplitude (DA) or axial displacement of the apex of the cornea from the initial corneal state, central radius of the cornea (R), integrated radius (IR), deformation amplitude ratio (DAR = DA at the apex/average of DA at 2 mm around the center in the two horizontal directions), and stiffness parameter at first applanation (SP-A1). In addition, two screening parameters of KCN were recorded to assess their detection ability, one is the combination of DCR parameters and corneal thickness profile in the horizontal meridian (CBI: Corvis biomechanical index), and the second is the tomographic biomechanical index (TBI). This index is calculated by combining tomographic data from Pentacam with corneal biomechanical data obtained using Corvis ST. This combination was performed using an artificial intelligence approach to improve the sensitivity and specificity of ectasia risk detection.

Corneal biomechanical parameters using ORA were corneal hysteresis (CH) and corneal resistance factor (CRF).

An image of the printout of Corvis ST and ORA showing the variables of interest extracted for this study is shown in Supplemental Fig. S2.

All corneal imaging techniques were performed by the same skilled technician under the supervision of an experienced optometrist. In the case of Corvis ST images, only records with a quality specification of "OK" were used for analysis. And in the case of the ORA, the reliability of the recorded signal was assessed based on the waveform score (WS) provided by the device. A WS of at least 3.5 was considered reliable [16].

Statistical analysis

Data were analyzed in SPSS.22 software (SPSS, Chicago, IL) after assessing the normality of quantitative data using the Kolmogorov-Smirnov test. The independent samples T-test was used to compare corneal biomechanical parameters between the two groups. A general linear model was used to compare corneal biomechanical parameters obtained from Corvis ST and ORA in normal and subclinical keratoconus groups, while central corneal thickness (CCT) and biomechanically corrected intraocular pressure (bIOP) were considered covariates. Sensitivity and specificity for the best cut-off point of each corneal biomechanical parameter for the differential diagnosis of ACE-NT eyes from normal eyes were determined using receiver operating characteristic (ROC) curves. In addition, the area under the ROC curve (AUC) and Youden index for all corneal biomechanical parameters were determined. The significance level was considered as $p < 0.05$ in all tests. DeLong et al. method was used for the pairwise comparison of the AUCs for some corneal biomechanical parameters [17]. Here, Bonferroni correction was used and a P value less than 0.002 was considered statistically significant because pairwise comparisons were performed on 28 pairs.

RESULTS

In the normal group, 64 eyes (47.8%) belong to males and 70 eyes (52.2%) to females, and in the ACE-NT group 74 (57.8%) and 54 eyes (42.2%) to females and males, respectively. There was no statistically significant difference in the sex distribution between the two groups. ($P = 0.169$) The mean age of the normal and ACE-NT groups was 25.3 ± 3.5 years (age range 20–36 years) and 26.2 ± 4.3 years (range 19–35 years), respectively with no statistically significant difference. ($P = 0.450$)

The mean and standard deviation of the average keratometry and maximum keratometry (K_{max}) using Pentacam and TMS-4, I-S value, CCT, and bIOP in the ACE-NT versus normal groups are shown in Table 1.

The mean and standard deviation of corneal biomechanical parameters assessed using Corvis ST and ORA and combined parameters separately in the two groups while the central corneal thickness and biomechanically corrected intraocular pressure were

Table 1. Mean and standard deviation of average and maximum keratometry readings, inferior-superior asymmetry, corneal thickness, and biOP in two groups.

Variable	Mean \pm SD (95% CI)		P value
	ACE-NT (<i>n</i> = 128 eyes)	Normal (<i>n</i> = 134 eyes)	
Pentacam Front Mean KR (D)	43.78 \pm 1.56 (43.51–44.06)	43.63 \pm 1.39 (43.39–43.87)	0.395
Pentacam Front K_{max} (D)	45.17 \pm 1.47 (44.91–45.43)	44.62 \pm 1.38 (44.38–44.86)	0.001
TMS-4 Mean KR (D)	44.01 \pm 1.59 (43.73–44.28)	43.74 \pm 1.39 (43.30–43.77)	0.114
I-S value (D)	0.25 \pm 0.78 (0.11–0.38)	0.03 \pm 0.48 (–0.05 to 0.11)	0.006
CCT (μ m)	508.83 \pm 29.82 (503.61–514.04)	552.73 \pm 23.69 (548.68–556.78)	0.040
biOP (mmHg)	14.55 \pm 2.86 (14.05–15.05)	14.74 \pm 1.92 (14.41–15.07)	0.539

n = 262 eyes.

SD standard deviation, CI confidence interval, ACE-NT asymmetric contralateral corneal ectasia with normal topography, KR keratometry reading, K_{max} maximum keratometry, I-S inferior-superior asymmetry value, CCT central corneal thickness, biOP biomechanically corrected intraocular pressure.

considered as covariates along with the discriminative abilities of these parameters are displayed in Table 2.

There was a statistically significant difference in all corneal biomechanical parameters assessed using Corvis ST and ORA except for the first ($P = 0.865$) and second ($P = 0.226$) applanation lengths and deformation amplitude ($P = 0.936$) between the two groups.

Among the Corvis ST parameters, PD, HCR, and SPA1 had lower values in the ACE-NT group, while the values of IR, DAR, CBI, and TBI were lower in the normal eyes group. The highest and lowest differences between the two groups were related to SPA1 and AL1 & DA, respectively.

Among the parameters with significant differences, the highest effect size was related to TBI (0.402) and in a decreasing order related to CBI (0.18), AV2 (0.12), IR (0.06), PD (0.05), HCR (0.03), DAR (0.03), SPA1 (0.02), AV1 (0.02), CH (0.02), CRF (0.02), AL2 (0.01), DA (0.00), AL1 (0.00).

The highest and lowest accuracy of the classical parameters of Corvis ST were related to the radius of curvature at the highest concavity phase and the velocity during the second applanation phase with AUC, sensitivity, specificity 0.766, 70.31%, 77.61%, and 0.522, 62.50%, 44.03%, respectively.

The AUCs of the new Corvis ST parameters (SPA1, IR, and DAR) were higher than 0.84. Combined Corvis ST indices had higher accuracy based on AUC, sensitivity, and specificity compared to other DCR parameters as well as ORA parameters.

Considering all parameters, the best accuracy was observed for TBI with AUC 0.966, sensitivity 87.50%, and specificity 97.01% for cut-off point 0.24, respectively, and then for CBI with AUC 0.924, sensitivity and specificity 75.0% and 97.76% for a cut-off point 0.17, respectively.

ROC curves of some corneal biomechanical parameters using Corvis ST and ORA are illustrated in Fig. 1.

A pairwise comparison of the areas under the curve (AUC) associated with the 95% confidence interval (CI) for some corneal biomechanical indices is shown in Table 3.

The P value < 0.002 based on Bonferroni correction was considered statistically significant according to 21 pairwise comparisons here. The newer Corvis ST parameters did not show a significant difference in AUC with the pressure-derived indices of ORA. According to the combined parameters, there was a significant difference in AUC between TBI with CH ($P < 0.001$) and CRF ($P < 0.001$), and only between CBI with CH ($P < 0.001$).

DISCUSSION

Comparison of corneal biomechanical parameters assessed using Corvis ST and ORA in the normal group and asymmetric contralateral cornea ectasia with normal topography (ACE-NT) eyes showed a statistically significant difference in all parameters

except applanation lengths and deformation amplitude between the two groups. Among the parameters with significant differences, the highest effect size was related to TBI. The discriminative ability of composite/combined Corvis ST indices (TBI and CBI) was higher than other DCR parameters as well as ORA parameters, and among all parameters, the best accuracy was observed for TBI with AUC, sensitivity, and specificity of 0.966, 87.50%, and 97.01%, respectively.

Although several studies have investigated the diagnostic ability of corneal biomechanical parameters obtained using Corvis ST and ORA, further studies in different ethnicities are needed to confirm the results for their clinical implications, especially in refractive surgery centers. A summary of the literature review [15, 18–36] is presented in Table 4.

Only a few studies evaluated the discriminative ability of ORA parameters and only one study performed a similar study using both devices but in a very small sample size (ACE-NT, $n = 15$ eyes). While the present study assessed the diagnostic ability of corneal biomechanical parameters to distinguish normal from ACE-NT eyes in a larger sample ($n = 128$ eyes) using both available clinical devices for in vivo assessment of corneal biomechanical parameters to provide further evidence for the clinical use of these parameters.

In the study by Vincigura et al. for the differential diagnosis of the normal from definite/clinical keratoconus eyes using CBI as a combined index of Corvis ST, a sensitivity of 94.1% and a specificity of 100% were reported for the cut-off point of 0.50 [6]. Contrary to their study, the present study evaluated ACE-NT eyes versus distinct keratoconus, and a sensitivity and specificity of 75% and 97.8%, respectively, for the best cut-off point of 0.17 for CBI. Furthermore, in the current study, the best discriminability was seen for TBI (cut-off point 0.24, sensitivity 87.5%, and specificity 97.01%) as a combined biomechanical and topographical parameter, while CBI was the second parameter with the highest accuracy among other biomechanical parameters.

Other studies also reported high sensitivity and specificity for differentiation between healthy eyes and keratoconus eyes for CBI as well as DAR, IR, and SPA1 [37, 38]. Koh et al. in evaluating the correlation between Corvis ST corneal biomechanical parameters and the stages of keratoconus reported CBI as a useful index in the early detection of the initial stage of this disease [39]. The present findings confirmed their report in larger ACE cases (128 versus 53 eyes). In another study that is consistent with the result obtained in the present study, TBI was a better parameter to differentiate between the normal and keratoconus eyes (cut-off point 0.33, sensitivity 94.4%, and specificity of 94.9%) than other parameters assessed using Corvis ST [20], the lower cut-off point of 0.24 versus 0.33 in the current study is attributed to the difference in the type of keratoconus eyes assessed here.

Table 2. Mean and SD of corneal biomechanical parameters using Corvis ST and ORA separately in eyes with ACE-NT and normal groups and central corneal thickness and intraocular pressure as covariates along with ROC curve analysis.

Variables	Mean ± SD (95% CI)	P value	AUC (95% CI)	Youden index	Cut-off	Sen (%) (95% CI)	Sp (%) (95% CI)
	ACE-NT (n = 128 eyes)		Normal (n = 134 eyes)				
CorVis ST parameters							
AL1 (mm)	2.24 ± 0.31 (2.18–2.31)	0.865	0.636 (0.575–0.694)	0.2774	≤2.32	69.53 (60.8–77.4)	58.12 (49.4–66.7)
AL2 (mm)	1.62 ± 0.51 (1.53–1.71)	0.226	0.606 (0.544–0.665)	0.2435	≤1.18	43.75 (35.0–52.8)	80.60 (72.9–86.9)
AV1 (m/s)	0.13 ± 0.02 (0.13–0.14)	0.047	0.712 (0.653–0.766)	0.3758	>0.13	72.66 (64.1–80.2)	64.93 (56.2–73.0)
AV2 (m/s)	−0.32 ± 0.04 (−0.33 to −0.32)	<0.001	0.522 (0.459–0.583)	0.06530	≤−0.33	62.50 (53.5–70.9)	44.03 (35.5–52.9)
HC, PD (mm)	5.08 ± 0.31 (5.04–5.12)	<0.001	0.602 (0.540–0.662)	0.1877	>4.93	85.94 (78.7–91.4)	32.84 (25.0–41.5)
HC, R (mm)	7.09 ± 1.19 (6.89–7.29)	0.012	0.766 (0.710–0.816)	0.4792	≤7.15	70.31 (61.6–78.1)	77.61 (69.6–84.4)
HC, DA (mm)	1.07 ± 0.11 (1.06–1.09)	0.936	0.737 (0.679–0.789)	0.3598	>1.06	70.31 (61.6–78.1)	65.67 (57.0–73.7)
SP-A1 (mmHg/mm)	102.37 ± 15.36 (100.08–104.65)	0.037	0.838 (0.787–0.880)	0.5570	≤103.1	77.34 (69.1–84.3)	78.36 (70.4–85.0)
IR (mm ^{−1})	8.41 ± 1.42 (8.20–8.61)	<0.001	0.846 (0.796–0.887)	0.5798	>7.9	78.12 (70.0–84.9)	79.85 (72.1–86.3)
DAR	4.42 ± 0.54 (4.37–4.51)	0.004	0.846 (0.796 to 0.887)	0.5211	>4.2	80.47 (72.5–86.9)	71.64 (63.2–79.1)
CBI	0.45 ± 0.39 (0.40–0.50)	<0.001	0.924 (0.885–0.953)	0.7276	>0.17	75.00 (66.6–82.2)	97.76 (93.6–99.5)
TBI	0.63 ± 0.36 (0.56–0.67)	<0.001	0.966 (0.937–0.985)	0.8451	>0.24	87.50 (80.5–92.7)	97.01 (92.5–99.2)
ORA parameters							
CH (mmHg)	9.94 ± 1.33 (9.71–10.17)	0.008	0.825 (0.773–0.869)	0.5176	≤9.9	72.66 (64.1–80.2)	79.10 (71.2–85.6)
CRF (mmHg)	9.58 ± 1.66 (9.37–9.80)	0.002	0.866 (0.819–0.905)	0.6028	≤9.6	79.69 (71.7–86.3)	80.60 (72.9–86.9)

n = 262 eyes. SD standard deviation, AUC area under the curve, Sen sensitivity, Sp specificity, CI confidence interval, ACE-NT asymmetric contralateral corneal ectasia with normal topography, AL applanation length, AV applanation velocity, HC highest concavity, PD peak distance, R radius of curvature, DA deformation amplitude, SP-A1, stiffness parameter at first applanation, IR integrated radius, DAR deformation amplitude ratio, CBI corvis biomechanical index, TBI tomographic biomechanical index, CH corneal hysteresis, CRF corneal resistance factor.

The present cut-off point is very similar to the study of Ambrosio and colleagues who reported a cut-off point of 0.29 with AUC, sensitivity, and specificity of 0.822, 90.4%, and 96% for TBI as a sensitive parameter for the diagnosis of ACE [21]. One distinctive feature of the present study in comparison with their study is the inclusion of the pressure-derived of ORA other than Corvis ST in this diagnostic study.

A recent study introduced AV2 as an important parameter for the diagnosis of the initial stage of keratoconus [40], while in the present study, unlike their study, AV2 showed low detection ability

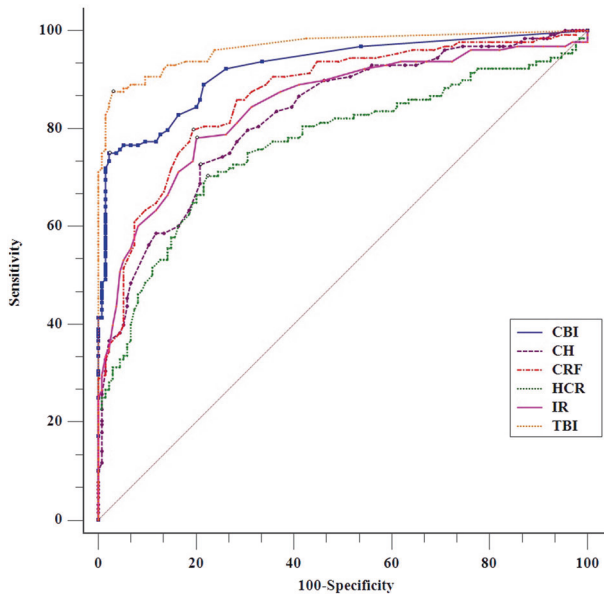


Fig. 1 Receiver operating characteristic (ROC) curves of some corneal biomechanical parameters using both devices in the ACE-NT (n = 128) and normal (n = 134) eyes. ACE-NT Asymmetric Contralateral Corneal Ectasia with Normal Topography, CBI Corvis Biomechanical Index, TBI Tomographic Biomechanical Index, HCR Radius of Curvature at the highest concavity, IR Integrated Radius, CH Corneal Hysteresis, CRF Corneal Resistance Factor.

based on AUC compared to DAR (0.846), IR (0.846), CBI (0.924), and TBI (0.966) or even the diagnostic ability of ORA parameters.

In assessing the detection ability of corneal biomechanical indices in a Chinese population, Ren et al. mentioned three parameters of SPA1, CBI, and IR (with AUC of 0.668) as parameters with higher diagnostic ability based on AUC 0.753, 0.703, and 0.668), respectively [18]; while the present study in a larger sample of the Iranian population found TBI and CBI as the parameters with the best detection capabilities.

Another work in line with the current work is a study by Wu et al., which also confirmed the high diagnostic ability of TBI for early detection of keratoconus [41], with the difference that the present study was performed on eyes with ACE-NT instead of clinical or definite keratoconus in their study. In addition, ORA parameters were examined to better evaluate the diagnostic function of corneal biomechanical parameters that are assessed clinically in vivo.

In assessing the performance of Corvis ST and ORA parameters, DA at the highest concavity phase and SPA1 were reported as indices with stronger detection ability, while CH and CRF did not enhance the diagnosis [19], while in the present study, although SPA1 had a higher ability compared to the standard Corvis ST parameter; its capability was lower than the combined indices (CBI & TBI) and on the other hand, CRF appeared as a parameter with an acceptable diagnostic ability. The most important reason for the difference between the present study and Zhang et al.'s work, in addition to racial differences, can be attributed to the evaluation of a much larger sample of VAE cases, which was approximately 8.5 times larger than in their study.

Low CH and CRF were reported in eyes with keratoconus eyes [42–44]; however, the current study confirmed these findings and showed cut-off points of 9.9 mmHg (72.66% sensitivity and 79.10% specificity) and 9.6 mmHg (79.69% sensitivity and 80.60% specificity) for differentiation between normal and ACE eyes with normal topography.

One limitation of this study was the failure to investigate parameters derived from the ORA response curve waveform. Evaluation of the diagnostic ability of corneal shape parameters along with different elements of the ABCD grading system of keratoconus in a large sample of eyes with ACE-NT is suggested for future research. In addition, monitoring the biomechanical

Table 3. Pairwise comparison of the areas under the curve (AUC) for some corneal biomechanical parameters assessed using Corvis ST and ORA.

Variables	Difference between AUCs (95% CI) p value					
	IR	DAR	CBI	TBI	CH	CRF
SPA1	0.01 (−0.05 to 0.07) P = 0.784	0.01 (−0.04 to 0.06) P = 0.762	0.09 (0.04–0.13) P < 0.001	0.13 (0.08–0.18) P < 0.001	0.01 (−0.05 to 0.07) P = 0.682	0.03 (−0.02 to 0.08) P = 0.270
IR	–	0.00 (−0.03 to 0.04) P = 0.990	0.08 (0.02–0.13) P = 0.007	0.12 (0.07–0.17) P < 0.001	0.02 (−0.04 to 0.08) P = 0.470	0.02 (−0.03 to 0.07) P = 0.432
DAR	–	–	0.08 (0.03– 0.13) P = 0.003	0.12 (0.07–0.17) P < 0.001	0.02 (−0.03 to 0.07) P = 0.446	0.02 (−0.02 to 0.06) P = 0.354
CBI	–	–	–	0.04 (0.01–0.08) P = 0.017	0.10 (0.04–0.15) P < 0.001	0.06 (0.01–0.11) P = 0.020
TBI	–	–	–	–	0.14 (0.09–0.19) P < 0.001	0.10 (0.05–0.15) P < 0.001
CH	–	–	–	–	–	0.04 (0.01–0.07) P = 0.011

n = 262 eyes.

AUC area under the curve, CI confidence interval, SP-A1 stiffness parameter at first applanation, IR integrated radius, DAR deformation amplitude ratio, CBI corvis biomechanical index, TBI tomographic biomechanical index, CH corneal hysteresis, CRF corneal resistance factor.

Table 4. Comparison of diagnostic ability of different corneal biomechanical parameters.

Study	Country	Device	Group	Parameters' diagnostic ability (AUC & Cut-off)
Ren et al. [18]	China	Corvis ST	SCKC (n = 100 eyes) vs. Normal (n = 100 eyes)	SP-A1 (0.753 & ≤107.30), CBI (0.703 & >0.05), IR (0.668 & >8.94)
Zhang et al. [19]	China	Corvis ST & ORA	FFKC (n = 15 eyes) vs. Normal (n = 50 eyes)	TBI (0.885 & >0.11), CBI (0.752 & >0.594), CH (0.728 & ≤10.3), SP-A1 (0.716 & ≤86.805), CRF (0.709 & ≤10.7)
Ferreira-Mendes et al. [20]	Brazil	Corvis ST	VAE-NT (n = 57 eyes) vs. Normal (n = 312 eyes)	TBI (0.960 & 0.295), CBI (0.775 & 0.005)
Ambrósio, Jr. et al. [21]	Brazil & Italy	Corvis ST	VAE-NT (n = 94 eyes) vs. Normal (n = 480 eyes)	TBI (0.985 & 0.29), CBI (0.822 & 0.07)
Koh et al. [15]	Japan	Corvis ST	VAE-NT (n = 23 eyes) vs. Normal (n = 70 eyes)	TBI (0.751 & 0.259), CBI (0.660 & -)
Luz et al. [22]	Brazil	ORA	FFKC (n = 21 eyes) vs. Normal (n = 76 eyes)	Neither CH nor CRF achieved statistically significant differences.
Catalán-López, et al. [23]	Spain	Corvis ST	VAE-NT (n = 18 eyes) vs. Normal (n = 100 eyes)	AL2 (0.69 & 1.48), HC-R (0.68 & 7.52), PD (0.67 & 4.93), Not include ARV printout parameters
Song et al. [24]	China	Corvis ST	SCKC (n = 89 eyes) vs. Normal (n = 105 eyes)	SPA1 (0.86 & 101.2), TBI (0.84 & 0.17), CBI (0.80 & 0.05)
Tian et al. [25]	China	Corvis ST	FFKC (n = 36 eyes) vs. Normal (n = 50 eyes)	SPA1 (0.710 & 88.191), CBI (0.684 & 0.039)
Liu et al. [26]	China	Corvis ST	VAE-NT (n = 27 eyes) vs. Normal (n = 79 eyes)	TBI (0.928 & 0.38), CBI (0.860 & 0.27)
Guo et al. [27]	China	Corvis ST	FFKC (n = 83 eyes) vs. Normal (n = 158 eyes)	SPA1 (0.761 & 96.71), TBI (0.722 & 0.273), DAR (0.712 & 4.464), CBI (0.667 & 0.067)
Heidari et al. [28]	Iran	Corvis ST	SCKC (n = 79 eyes) vs. Normal (n = 69 eyes)	TBI (0.828 & >0.39), SPA1 (0.779 & -), CBI (0.758 & -), IR (0.725 & -)
Zhang et al. [29]	China	Corvis ST	FFKC (n = 31 eyes) vs. Normal (n = 60 eyes)	CBI (0.909 & 0.019), TBI (0.899 & 0.225)
Koc et al. [30]	Turkey	Corvis ST	SCKC (n = 21 eyes) vs. Normal (n = 35 eyes)	TBI (0.790 & 0.29)
Chan et al. [31]	Hong Kong	Corvis ST	SCKC (n = 23 eyes) vs. Normal (n = 37 eyes)	TBI (0.925 & 0.16)
Wang et al. [32]	Hong Kong	Corvis ST	FFKC (n = 21 eyes) vs. Normal (n = 73 eyes of 38 subjects)	CBI (0.785 & -)
Kataria et al. [33]	India	Corvis ST	VAE-NT (n = 100 eyes) vs. Normal (n = 100 eyes)	TBI (0.825 & 0.09), CBI (0.678 & 0.01), SPA1 (0.655 & ≤93.61)
Kirgiz et al. [34]	Turkey	ORA	FFKC (n = 50 eyes) vs. Normal (n = 50 eyes)	CRF (0.90 & 9.25), CH (0.85 & 9.45)
Galletti et al. [35]	Argentina	ORA	SCKC (n = 73 eyes) vs. Normal (n = 87 eyes)	CRF (0.84 & <8.46), CH (0.71 & <9.19)
Kozobolis et al. [36]	Greece	ORA	FFKC (n = 50 eyes) vs. Normal (n = 50 eyes)	CRF (0.9154 & 9.9), CH (0.826 & 10.8)
Current study	Iran	Corvis ST & ORA	ACE-NT (n = 128 eyes) vs. Normal (n = 134 eyes)	TBI (0.966 & >0.24), CBI (0.924 & >0.17), CRF (0.866 & ≤9.6), IR (0.846 & >7.9), DAR (0.846 & >4.2), SP-A1 (0.838 & ≤103.1), CH (0.825 & ≤9.9)

AUC area under the curve, ORA ocular response analyzer, SCKC subclinical keratoconus, FFKC forme fruste keratoconus, ACAE-NT asymmetric contralateral corneal ectasia with normal topography, AL applanation length, HC-R highest concavity radius, PD peak distance, SP-A1 stiffness parameter at first applanation, IR integrated radius, DAR deformation amplitude ratio, CBI corvis biomechanical index, TBI tomographic biomechanical index, CH corneal hysteresis, CRF corneal resistance factor.

changes of ACE-NT eyes over time using the new BEST Display (Homburg Biomechanical E-STaging Display) is another area of interest for future studies.

In conclusion, the present study in comparison of corneal biomechanical parameters using Corvis ST and ORA assessed in a large group of eyes with asymmetric contralateral ectasia with normal corneal topography showed that all parameters enable to differentiate between the two groups except applanation lengths and deformation amplitude. The highest accuracy (AUC) among the classic, new, and combined parameters of Corvis ST were related to the radius of curvature at HC phase (0.766), IR & DAR (0.846), and CBI (0.24) & TBI (0.966), respectively. Using ORA, CRF (AUC: 0.866) had a higher detection ability than CH (AUC: 0.826). Among all parameters with significant differences, the highest effect sizes were related to TBI (0.402) and CBI (0.18). Overall, the best accuracy was obtained for TBI, with a cut-off point of 0.24, a sensitivity of 87.50%, and a specificity of 97.01% for the differential diagnosis of normal eyes from very asymmetric ectasia with normal corneal topography.

SUMMARY

What was known before

- Assessing the corneal biomechanical properties appear as one of the main approaches in the early detection of keratoconus.

What this study adds

- TBI has the best accuracy and the highest effect size for differential diagnosis of normal eyes from the eyes with asymmetric contralateral corneal ectasia with normal topography (ACE-NT) with a cut-off point 0.24.
- The corneal resistance factor (CRF) had a higher detection ability than corneal hysteresis (CH).

DATA AVAILABILITY

All data generated or analyzed during this study are included in this published article [and its supplementary information files].

REFERENCES

- Ucar M, Cakmak HB, Sen B. A statistical approach to classification of keratoconus. *Int J Ophthalmol*. 2016;9:1355–7.
- Serdarogullari H, Tetikoglu M, Karahan H, Altin F, Elcioglu M. Prevalence of keratoconus and subclinical keratoconus in subjects with astigmatism using pentacam derived parameters. *Ophthalmic Vis Res*. 2013;8:213–9.
- Feizi S, Yaseri M, Kheiri B. Predictive ability of galilei to distinguish subclinical keratoconus and keratoconus from normal corneas. *Ophthalmic Vis Res*. 2016;11:8–16.
- Huseynli S, Abdullalalyeva F. Evaluation of scheimpflug tomography parameters in subclinical keratoconus, clinical keratoconus and normal caucasian eyes. *Turk J Ophthalmol*. 2018;48:99–108.
- Fontes BM, Ambrosio R Jr., Velarde GC, Nose W. Corneal biomechanical evaluation in healthy thin corneas compared with matched keratoconus cases. *Arq Bras Oftalmol*. 2011;74:13–16.
- Vinciguerra R, Ambrosio R Jr., Elsheikh A, Roberts CJ, Lopes B, Morengi E, et al. Detection of keratoconus with a new biomechanical index. *J Refract Surg*. 2016;32:803–10.
- Tian L, Ko MW, Wang LK, Zhang JY, Li TJ, Huang YF, et al. Assessment of ocular biomechanics using dynamic ultra high-speed Scheimpflug imaging in keratoconic and normal eyes. *J Refract Surg*. 2014;30:785–91.
- Roberts CJ, Dupps WJ Jr. Biomechanics of corneal ectasia and biomechanical treatments. *J Cataract Refract Surg*. 2014;40:991–8.
- Sedaghat MR, Momeni-Moghaddam H, Roberts CJ, Maddah N, Ambrósio R Jr., Hosseini SR. Corneal biomechanical parameters in keratoconus eyes with

abnormal elevation on the back corneal surface only versus both back and front surfaces. *Sci Rep*. 2021;11:11971.

- Tabbara KF, Kotb AA. Risk factors for corneal ectasia after LASIK. *Ophthalmology*. 2006;113:1618–22.
- Li Y, Chamberlain W, Tan O, Brass R, Weiss JL, Huang D. Subclinical keratoconus detection by pattern analysis of corneal and epithelial thickness maps with optical coherence tomography. *J Cataract Refract Surg*. 2016;42:284–95.
- de Sanctis U, Loiacono C, Richiardi L, Turco D, Mutani B, Grignolo FM. Sensitivity and specificity of posterior corneal elevation measured by Pentacam in discriminating keratoconus/subclinical keratoconus. *Ophthalmology*. 2008;115:1534–9.
- Moshirfar MMM, Murri MS, Momeni-Moghaddam H, Ronquillo YC, Hoopes PC. Advances in biomechanical parameters for screening of refractive surgery candidates a review of the literature, Part III. *Med Hypothesis Discov Innov Ophthalmol*. 2019;8:219–40.
- Sedaghat MR, Momeni-Moghaddam H, Yekta A, Elsheikh A, Khabazkhoob M, Ambrosio R Jr, et al. Biomechanically-corrected intraocular pressure compared to pressure measured with commonly used tonometers in normal subjects. *Clin Optom*. 2019;11:127–33.
- Koh S, Ambrósio R Jr., Inoue R, Maeda N, Miki A, Nishida K. Detection of subclinical corneal ectasia using corneal tomographic and biomechanical assessments in a Japanese population. *J Refract Surg*. 2019;35:383–90.
- Momeni-Moghaddam H, Hashemi H, Zarei-Ghanavati S, Ostadimoghaddam H, Yekta A, Aghamirsalim M, et al. Four-year changes in corneal biomechanical properties in children. *Clin Exp Optom*. 2019;102:489–95.
- DeLong ER, DeLong DM, Clarke-Pearson DL. Comparing the areas under two or more correlated receiver operating characteristic curves: a nonparametric approach. *Biometrics*. 1988;44:837–45.
- Ren S, Xu L, Fan Q, Gu Y, Yang K. Accuracy of new Corvis ST parameters for detecting subclinical and clinical keratoconus eyes in a Chinese population. *Sci Rep*. 2021;11:4962.
- Zhang H, Tian L, Guo L, Qin X, Zhang D, Li L, et al. Comprehensive evaluation of corneas from normal, forme fruste keratoconus and clinical keratoconus patients using morphological and biomechanical properties. *Int Ophthalmol*. 2021;41:1247–59.
- Ferreira-Mendes J, Lopes BT, Faria-Correia F, Salomão MQ, Rodrigues-Barros S, Ambrósio R Jr. Enhanced ectasia detection using corneal tomography and biomechanics. *Am J Ophthalmol*. 2019;197:7–16.
- Ambrósio R Jr., Lopes BT, Faria-Correia F, Salomão MQ, Bühren J, Roberts CJ, et al. Integration of scheimpflug-based corneal tomography and biomechanical assessments for enhancing ectasia detection. *J Refract Surg*. 2017;33:434–43.
- Luz A, Lopes B, Hallahan KM, Valbon B, Fontes B, Schor P, et al. Discriminant value of custom ocular response analyzer waveform derivatives in forme fruste keratoconus. *Am J Ophthalmol*. 2016;164:14–21.
- Catalán-López S, Cadarso-Suárez L, López-Ratón M, Cadarso-Suárez C. Corneal biomechanics in unilateral keratoconus and fellow eyes with a scheimpflug-based tonometer. *Optom Vis Sci*. 2018;95:608–15.
- Song P, Ren S, Liu Y, Li P, Zeng Q. Detection of subclinical keratoconus using a novel combined tomographic and biomechanical model based on an automated decision tree. *Sci Rep*. 2022;12:5316.
- Tian L, Zhang D, Guo L, Qin X, Zhang H, Zhang H, et al. Comparisons of corneal biomechanical and tomographic parameters among thin normal cornea, forme fruste keratoconus, and mild keratoconus. *Eye Vis*. 2021;8:44.
- Liu Y, Zhang Y, Chen Y. Application of a scheimpflug-based biomechanical analyser and tomography in the early detection of subclinical keratoconus in chinese patients. *BMC Ophthalmol*. 2021;21:339.
- Guo LL, Tian L, Cao K, Li YX, Li N, Yang WQ, et al. Comparison of the morphological and biomechanical characteristics of keratoconus, forme fruste keratoconus, and normal corneas. *Semin Ophthalmol*. 2021;36:671–8.
- Heidari Z, Hashemi H, Mohammadpour M, Amanzadeh K, Fotouhi A. Evaluation of corneal topographic, tomographic and biomechanical indices for detecting clinical and subclinical keratoconus: a comprehensive three-device study. *Int J Ophthalmol*. 2021;14:228–39.
- Zhang M, Zhang F, Li Y, Song Y, Wang Z. Early diagnosis of keratoconus in chinese myopic eyes by combining corvis ST with Pentacam. *Curr Eye Res*. 2020;45:118–23.
- Koc M, Aydemir E, Tekin K, Inanc M, Kosekahya P, Kiziltoprak H. Biomechanical analysis of subclinical keratoconus with normal topographic, topometric, and tomographic findings. *J Refract Surg*. 2019;35:247–52.
- Chan TCY, Wang YM, Yu M, Jhanji V. Comparison of corneal tomography and a new combined tomographic biomechanical index in subclinical keratoconus. *J Refract Surg*. 2018;34:616–21.
- Wang YM, Chan TCY, Yu M, Jhanji V. Comparison of corneal dynamic and tomographic analysis in normal, forme fruste keratoconic, and keratoconic eyes. *J Refract Surg*. 2017;33:632–8.

33. Kataria P, Padmanabhan P, Gopalakrishnan A, Padmanaban V, Mahadik S, Ambrósio R Jr. Accuracy of Scheimpflug-derived corneal biomechanical and tomographic indices for detecting subclinical and mild keratectasia in a South Asian population. *J Cataract Refract Surg.* 2019;45:328–36.
34. Kirgiz A, Karaman Erdur S, Atalay K, Gurez C. The role of ocular response analyzer in differentiation of forme fruste keratoconus from corneal astigmatism. *Eye Contact Lens.* 2019;45:83–87.
35. Galletti JD, Ruiseñor Vázquez PR, Fuentes Bonthoux F, Pfortner T, Galletti JG. Multivariate analysis of the ocular response analyzer's corneal deformation response curve for early keratoconus detection. *J Ophthalmol.* 2015;2015:496382.
36. Kozobolis V, Sideroudi H, Giarmoukakis A, Gkika M, Labiris G. Corneal biomechanical properties and anterior segment parameters in forme fruste keratoconus. *Eur J Ophthalmol.* 2012;22:920–30.
37. Vinciguerra R, Ambrósio R, Elsheikh A, Roberts CJ, Lopes B, Morengi E, et al. Detection of keratoconus with a new biomechanical index. *J Refractive Surg.* 2016;32:803–10.
38. Sedaghat MR, Momeni-Moghaddam H, Ambrósio R Jr, Heidari HR, Maddah N, Danesh Z, et al. Diagnostic ability of corneal shape and biomechanical parameters for detecting frank keratoconus. *Cornea.* 2018;37:1025–34.
39. Koh S, Inoue R, Ambrósio R, Jr, Maeda N, Miki A, Nishida K. Correlation between corneal biomechanical indices and the severity of keratoconus. *Cornea.* 2019;00:1–7.
40. Perez-Rueda A, Jimenez-Rodriguez D, Castro-Luna G. Diagnosis of subclinical keratoconus with a combined model of biomechanical and topographic parameters. *J Clin Med.* 2021;10:2746.
41. Wu Y, Guo LL, Tian L, Xu ZQ, Li Q, Hu J, et al. Comparative analysis of the morphological and biomechanical properties of normal cornea and keratoconus at different stages. *Int Ophthalmol.* 2021;41:3699–711.
42. Fontes BM, Ambrósio R Jr., Jardim D, Velarde GC, Nosé W. Corneal biomechanical metrics and anterior segment parameters in mild keratoconus. *Ophthalmology.* 2010;117:673–9.
43. Pinero DP, Alcon N. In vivo characterization of corneal biomechanics. *J Cataract Refract Surg.* 2014;40:870–87.
44. Shah S, Laiquzzaman M, Bhojwani R, Mantry S, Cunliffe I. Assessment of the biomechanical properties of the cornea with the ocular response analyzer in normal and keratoconic eyes. *Investig Ophthalmol Vis Sci.* 2007;48:3026–31.

ACKNOWLEDGEMENTS

The authors would like to thank the personnel of Didar eye clinic and the participants who made this study possible.

AUTHOR CONTRIBUTIONS

All authors contributed to data analysis, drafting or revising the article, gave final approval of the version to be published, and agree to be accountable for all aspects of the work.

COMPETING INTERESTS

The authors declare no competing interests.

ETHICS APPROVAL

This research was approved by the Ethics Committee of the Deputy of Research of Mashhad University of Medical Sciences (Code: IR.MUMS.REC.1399.418).

ADDITIONAL INFORMATION

Supplementary information The online version contains supplementary material available at <https://doi.org/10.1038/s41433-022-02218-9>.

Correspondence and requests for materials should be addressed to Hamed Momeni-Moghaddam.

Reprints and permission information is available at <http://www.nature.com/reprints>

Publisher's note Springer Nature remains neutral with regard to jurisdictional claims in published maps and institutional affiliations.

Springer Nature or its licensor holds exclusive rights to this article under a publishing agreement with the author(s) or other rightsholder(s); author self-archiving of the accepted manuscript version of this article is solely governed by the terms of such publishing agreement and applicable law.